*J. Biochem.* **134**, 615–623 (2003)
DOI: 10.1093/jb/mvg184

# Patch Clamp Analysis of a H$^+$ Pump Heterologously Expressed in Giant Yeast Vacuoles

**Yoichi Nakanishi[1], Isamu Yabe[2] and Masayoshi Maeshima[*,1]**

*[1]Laboratory of Cell Dynamics, Graduate School of Bioagricultural Sciences, Nagoya University, Nagoya 464-8601; and [2]the Institute of Molecular and Cellular Biosciences, the University of Tokyo, Tokyo 113-0032*

Received June 17, 2003; accepted August 21, 2003

**Despite the usefulness of the patch-clamp technique, its application to ion pumps and transporters in biomembranes is limited. We developed a novel method for determining the activity of a proton-pumping pyrophosphatase (H$^+$-PPase) made of a single protein. We heterologously highly expressed the enzyme in *Saccharomyces cerevisiae*, prepared giant vacuoles from the cells, and measured a PPi-dependent electrical current of 18 pA (10.5 fA/μm$^2$) using the patch-clamp technique in the whole-vacuole recording mode. We determined the inhibitor sensitivity and affinity for substrate ($K_m$, 4.6 μM). The enzyme number in a giant vacuole ($4.2 \times 10^6$) and the molecular activity of the expressed H$^+$-PPase (14 s$^{-1}$) were determined. An uncoupling-type H$^+$-PPase mutant, of which the 263rd glutamate residue was replaced by aspartate, and of which H$^+$ pump activity was not detected with the fluorescence quenching method, showed a weak current with a high $K_m$. The high accuracy, effectiveness and applicability of the method for exogenously expressed ion transporters were also discussed.**

**Key words: H$^+$ current, H$^+$-pyrophosphatase, patch-clamp, proton pump, vacuole.**

Abbreviations: H$^+$-PPase, H$^+$-translocating inorganic pyrophosphatase; V-ATPase, vacuolar H$^+$-ATPase.

The patch-clamp technique allows the flow and the direction of electrical currents through biological membranes to be analyzed in real-time (*1–4*). With this technique, many ion channels have been studied as to their molecular physiology, however, it has been difficult to analyze the activities of ion pumps and transporters. First, the transport rates of pumps (10–$10^2$ s$^{-1}$) and transporters ($10^2$–$10^3$ s$^{-1}$) are slow compared to ion channels. Typically, channels transport ions at rates of $10^6$ to $10^8$ s$^{-1}$. An electrical current of >1 pA is essential for quantitative analysis. A current of 1 pA for a monovalent ion equates to a transport rate of $6 \times 10^6$ s$^{-1}$. Therefore, ion currents can only be obtained as the sum of the activity of many pumps or transporters. Second, the catalytic site of pumps is often exposed to the cytosolic face that is connected to the pipette buffer in the whole-cell recording mode. It is hard to quickly change the pipette buffer. By patch clamping of the excised inside-out membrane, the functional domain can be exposed to the bathing medium, but the membrane surface area is too small to measure the required number of transporters.

The activities of endogenous ion pumps have been determined by engineering *Escherichia coli* with giant vacuole-like structures (provacuoles: prokaryotic vacuoles) using the spheroplast incubation method (*5*). This method was subsequently used to prepare oversized vacuoles in *Saccharomyces cerevisiae* cells, and the H$^+$ current of endogenous vacuolar H$^+$-ATPase (V-ATPase) was measured using the whole-vacuole clamp technique (*6*). This method has been expected to be used for determining the activities of various ion pumps and ion transporters, which are heterologously expressed in *E. coli* and yeast cells, using the patch-clamp technique.

In the present study, plant vacuolar H$^+$-pyrophosphatase (H$^+$-PPase) was introduced into *S. cerevisiae* in order to characterize its activity. H$^+$-PPase is found in plants, parasitic protists such as the malarial parasite, some eubacteria and archaebacteria (*7–14*). Yeast and animal cells are devoid of the enzyme. This enzyme translocates H$^+$ across membrane, coupled with the hydrolysis of inorganic pyrophosphate ($PP_i$), generating a pH gradient (*15*). The enzymatic function of H$^+$-PPase is performed by a single polypeptide of 80 kDa, which exists as a homodimer in the vacuolar membrane. Furthermore, the substrate also has a simple structure. Thus, H$^+$-PPase should be a good model for studying proton pumps (*9*, *16*). The catalytic site of the enzyme is exposed to the cytosol, *via* which the substrate PPi is supplied. At least two cytosolic domains that contain a consensus sequence were demonstrated to be essential for the catalytic function by site-directed mutagenic analysis (*17*). We cannot determine the detailed mechanism and structure-function relationship between PPi-hydrolysis and H$^+$ translocation without quantitative and real-time determination of the function. Here we developed methods for producing H$^+$-PPase in *S. cerevisiae* at high levels and for preparing enlarged vacuoles, and applied the patch-clamp technique to determine the H$^+$ current caused by the enzyme in isolated intact yeast vacuoles. It has been demonstrated that this method can be used to characterize mutant enzymes.

[*]To whom correspondence should be addressed. Tel/Fax: +81-52-789-4096, E-mail: maeshima@agr.nagoya-u.ac.jp

 

## EXPERIMENTAL PROCEDURES

*Strains and Plasmids*—We prepared plasmid pYN10 by deleting the promoter region of the *URA3* marker gene (resulting *ura3*-d allele) of a yeast expression vector, pKT10 (*17*, *18*). With the pYN10 plasmid, the plasmid copy number and the expression level of proteins in yeast were five times greater than those for the original plasmid pKT10. cDNAs for mung bean $H^+$-PPase (*19*) and its mutants (*17*) were subcloned into pYN10. The DNA constructs of pYV1 (wild type $H^+$-PPase), pYV259A (V259A mutant), pYK261R (K261R), and pYE263D (E263D) were introduced into *S. cerevisiae* strain BJ5458 (*Mat α, ura3-52, trp1, lys2-801, leu2Δ1, his3Δ200, pep4::HIS3, prbΔ1.6R can1, GAL*) (*17*, *20*).

*Preparation of Giant Yeast Cells*—We prepared giant cells by the spheroplast incubation method (*6*) with the following modifications. *S. cerevisiae* was cultured in AHCW/Glc medium at 30°C (*17*). At the early log phase ($OD_{660}$ of 0.2), cells (1 ml) were incubated with 0.1 M Tris-HCl, pH 9.4, 50 mM 2-mercaptoethanol and 0.1 M glucose at 30°C for 10 min. The cells were then treated at 30°C for 15 min in a medium containing 1 mg/ml zymolyase 20T, 1 M sorbitol, 2% (w/v) glucose, 50 mM Tris-HCl, pH 7.5, 0.043% yeast nitrogen base without amino acids and ammonium sulfate, and 0.25× dropout solution composed of all amino acids and adenines (*17*). We washed these spheroplasts twice with AHCW/Glc/1 M sorbitol medium, and then re-cultured them at 30°C for 24 h in 4 ml of the same medium supplemented with 10 μg/ml Aculeacin A, an inhibitor of 1,3-β-glucan synthase, which is an enzyme involved in cell wall synthesis (*21*). We kept the giant spheroplasts at 20°C and used them within 36 h.

*Giant Vacuole Isolation and Patch-Clamp Recording*—Vacuoles were isolated from giant spheroplasts by the osmotic shock method with the following modifications (*6*). Spheroplasts were concentrated by floating centrifugation at 1,500 ×*g* for 5 min and then diluted with 20 volumes of a hypotonic solution (0.2 M sorbitol, 0.1 M KCl and 20 mM Tris-Mes, pH 7.5) in the recording chamber of the patch-clamp apparatus. Vacuoles released from spheroplasts were gently washed with a bathing solution (0.2 M sorbitol, 0.1 M KCl, 1 mM $MgCl_2$ and 10 mM Tris-Mes, pH 7.5). A patch pipette was gently applied to a vacuole in the bathing solution and the membrane patch disrupted with a high-voltage pulse. Currents were recorded in the whole-vacuole mode with an originally constructed apparatus, as described previously (*5*, *6*). All experiments were carried out using the standard patch-clamp technique at 25°C. Throughout this report, a positive current represents a positive charge ($H^+$) moving from the cytoplasm to the inside of a vacuole.

*Determination of the Amount of $H^+$-PPase in a Giant Vacuole*—We cultured yeast cells at 30°C for 24 h and then at 20°C for 24 h on a large scale (200 ml). Giant cells were prepared and giant vacuoles isolated according to the floating centrifugation method (*22*). The procedure for preparation of vacuoles from giant yeast cells was the same as for the methods described above. Giant spheroplasts were diluted with 20 volumes of a hypotonic solution comprising 12% (w/v) Ficoll-400, 20 μM *p*-amidinophenyl-methanesulfonyl fluoride and 2 μg/ml leupeptin. The suspension was overlaid with buffer B (bathing solution plus 20 μM *p*-amidinophenyl-methanesulfonyl fluoride and 2 μg/ml leupeptin) containing 8% Ficoll-400 (8%-B), and buffer B containing 1.2% Ficoll-400 (1.2%-B). After centrifugation at 50,000 ×*g* for 30 min, the interface between 1.2%-B and 8%-B was collected and resuspended in 8%-B. The suspension was overlaid with 4.8% Ficoll-400 (4.8%-B) and 1.2%-B. Intact vacuoles floated on the 4.8%-B layer after centrifugation at 50,000 ×*g* for 30 min. The vacuoles were counted using a hemocytometer and their diameters were determined under a microscope (BX-60; Olympus, Tokyo). The absolute amount of $H^+$-PPase in the vacuoles was quantified by immunoblotting with anti-$H^+$-PPase antibodies from the calibration curve for the purified $H^+$-PPase (*23*).

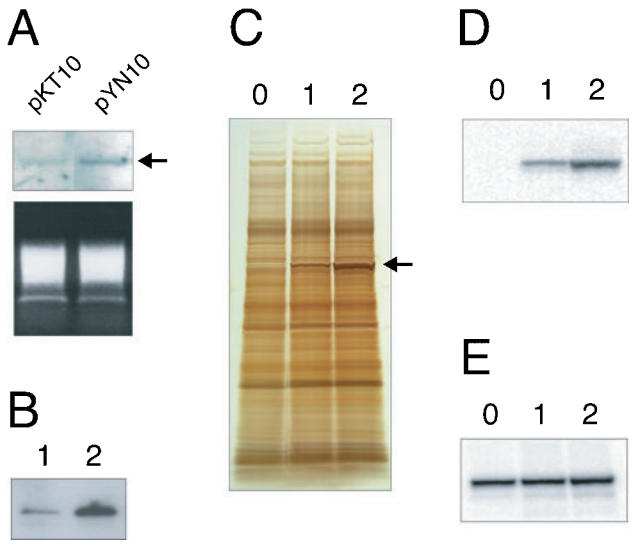


Fig. 1. **Enhanced heterologous expression of $H^+$-PPase in yeast cells using the pYN10 vector.** (A) Comparison of the accumulated amounts of plasmid DNAs of pKT10 and pYN10 vectors in *Saccharomyces serevisiae* cells (strain BJ5458). Aliquots (400 ng) of total DNA from yeast cells containing pKT10 or pYN10 were treated with *Eco*RI and then electrophoresed. Vector DNAs were detected by Southern hybridization (upper panel). DNAs in a gel were stained with ethidium bromide (lower panel). (B) Expression level of $H^+$-PPase protein (73 kDa) in yeast. Aliquots ($8 \times 10^4$ cells) of a total extract of BJ5458 containing pKVVP2 (pKT10 vector, lane 1) or pYV1 (pYN10 vector, lane 2) were subjected to SDS-PAGE and then subsequent immunoblot analysis with anti-$H^+$-PPase antibodies. (C–E) Comparison of the $H^+$-PPase protein levels in membranes. Membrane fractions were prepared from yeast BJ5458 cells containing the pYN10 vector (lane 0), pKVVP2 (lane 1) and pYV1 (lane 2). Aliquots (10 μg) were subjected to SDS-PAGE (C, the arrow indicates the position of $H^+$-PPase) and immunoblotting (D). (E) Amounts of endogenous 100-kDa subunit of V-ATPase in the membrane fractions.

## RESULTS

*High Level Expression of $H^+$-PPase in Yeasts*—We expressed the cDNA encoding $H^+$-PPase of mung bean (*Vigna radiata*) in *S. cerevisiae* strain BJ5458, which is deficient in major vacuolar proteinases (*17*). A new plasmid vector, pYN10, was constructed by deleting the promoter region of the *URA3* marker gene of a yeast expression vector, pKT10. With the pYN10 plasmid, the plasmid copy number increased, as shown in Fig. 1A. As a result,

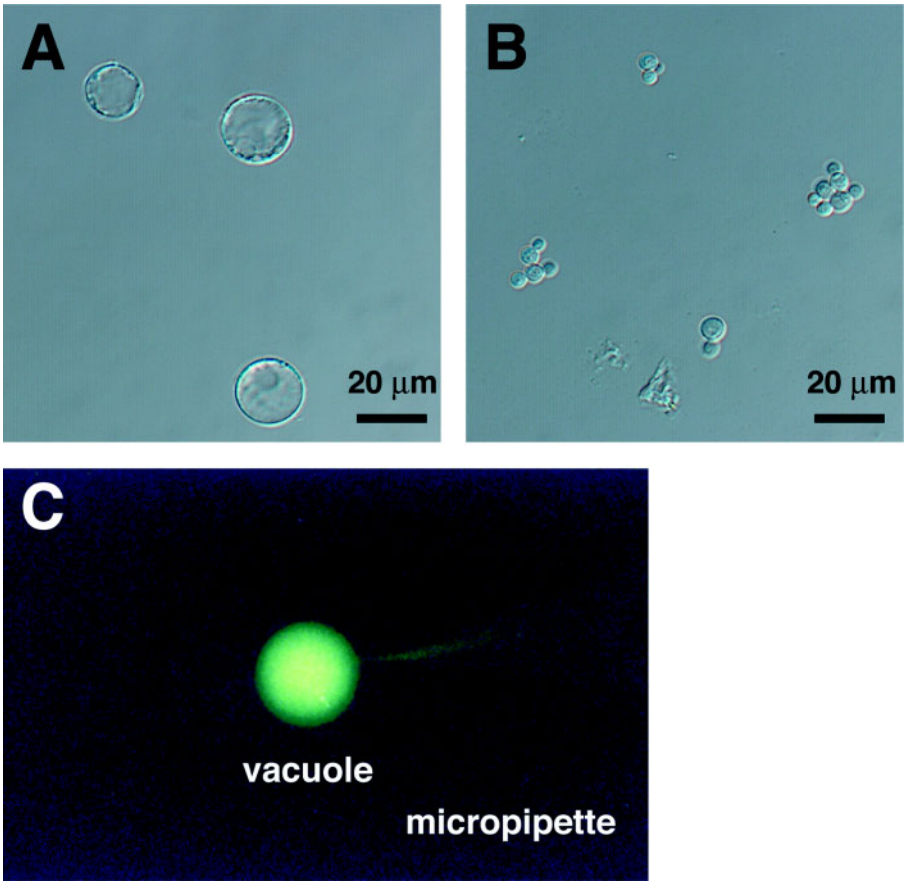


Fig. 2. **Giant-yeast cells and whole-vacuole configuration.** Giant cells of *Saccharomyces cerevisiae* BJ5458 pYV1 were obtained by the spheroplast incubation (SI) method. (A) Differential interference contrast (DIC) image of giant-yeast cells expressing H⁺-PPase. (B) DIC image of cells of the same strain (BJ5458 pYV1) grown without Aculeacin A. (C) Fluorescent image of the patch clamp in the whole-vacuole configuration. The membrane potential was clamped at 0 mV. The vacuole and a pipette were filled with the pipette buffer supplemented with carboxy-fluorescein to visualize their connection only for this demonstration.

the expression level of H⁺-PPase protein in yeast was five times greater than that of the original pKT10-based plasmid (Fig. 1, B, C, and D). The H⁺-PPase activity in the membrane fraction of yeast with a newly developed construct (pYV1) (160 ± 12 nmol/min/mg of membrane protein) was 5.5 times greater than that of the previous one (pKVVP2) (28.9 ± 1.4 nmol/min/mg), while the level of the 100-kDa subunit of yeast V-ATPase, an endogenous protein, was constant (Fig. 1E). Truncation of the promoter region of the *URA3* marker gene from another 2 μ plasmid vector has been reported to increase the plasmid copy number in yeast (*24*).

*Preparation of Giant Vacuoles Expressing H⁺-PPase*—We prepared giant cells of *S. cerevisiae* by the spheroplast incubation method (Fig. 2, A and B). Inhibition of cell wall synthesis is an essential point for generating giant yeast cells. As a specific inhibitor of cell wall synthesis, we used Aculeacin A instead of 2-deoxy glucose, which was used in the previous study (*6*). Aculeacins (A through G), lipopeptides produced by *Aspergillus aculeatus*, strongly inhibit 1,3-β-glucan synthase (*21*). When 2-deoxy glucose is used, glucose in the culture medium should be kept at a low concentration to generate giant yeast cells. V-PPase cDNA is not highly expressed with low concentrations of glucose, since the cDNA is linked with a glycelaldehyde-phosphate dehydrogenase (GAP) promoter, which is driven by glucose.

When giant spheroplasts prepared from giant cells are treated by moderate hypo-osmotic shock, only the plasma membranes are disrupted and vacuoles are released. A patch pipette is then attached to an isolated vacuole and the patch membrane is ruptured using a high voltage pulse. The vacuolar lumen is then connected to the pipette (whole-vacuole configuration) (Fig. 2C). We corrected for the capacitance of the vacuolar membrane, clamped the membrane potential at 0 mV, and monitored the total charge movement across the membrane.

*Patch-Clamp Recording of the H⁺ Current Generated by H⁺-PPase*—The whole-vacuole configuration was stable for over 2 h and we routinely recorded the H⁺ pump activity of the endogenous vacuolar V-ATPase. We detected a current of 30 pA at 1 mM ATP (Fig. 3A) caused by an influx of protons into the vacuole. The current produced by V-ATPase slowly decreased, with a half inactivation time of 8 min. In contrast to V-ATPase, a steady-state current of as high as 10 pA was formed after the addition of $PP_i$ to a concentration of 0.2 mM (Fig. 3A). H⁺-PPase retained over 90% of its activity for 2 h. A control vacuole, isolated from a cell transformed with a vector, did not generate a PPi-induced current, although an ATP-dependent current was recorded (Fig. 3B).

*Inhibition of the H⁺ Current by $PP_i$ Analogues and Metal Ions*—The H⁺ pump activity of H⁺-PPase is coupled with substrate hydrolysis, consequently the binding of a substrate to the enzyme does not cause H⁺ translocation. Indeed, the non-hydrolytic $PP_i$-analogues (*25*), imidodiphosphate and pamidronate, did not induce currents (Fig. 4A). These analogues competed with $PP_i$ and reversibly suppressed the $PP_i$-induced current. These data con-

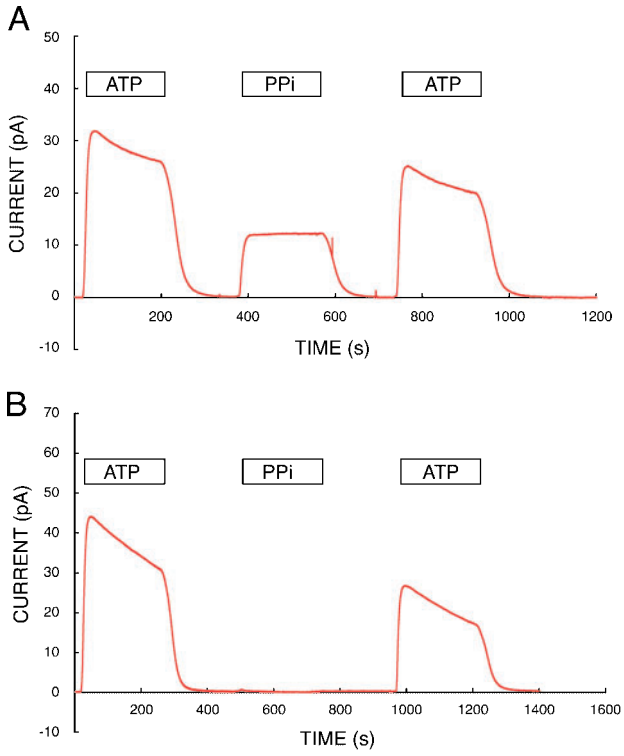


Fig. 3. **Current induced by $PP_i$ in a giant yeast vacuole containing $H^+$-PPase.** (A) ATP- and $PP_i$-induced currents in an intact vacuole expressing $H^+$-PPase. Both the bathing (cytoplasmic side) and pipette solutions (vacuolar lumen side) comprised 0.2 M sorbitol, 0.1M KCl, 10 mM Tris-Mes, pH 7.5, and 1 mM $MgCl_2$. The substrate, ATP (1 mM, at 1 and 13 min) or $PP_i$ (0.2 mM, at 7 min), was applied to the bathing solution at the indicated time for 3 min. During each interval, vacuoles were rinsed with buffer containing neither ATP nor $PP_i$. It took 30 s to exchange the bathing solution in a tube and chamber. (B) Vector control. The current of endogenous V-ATPase was observed.

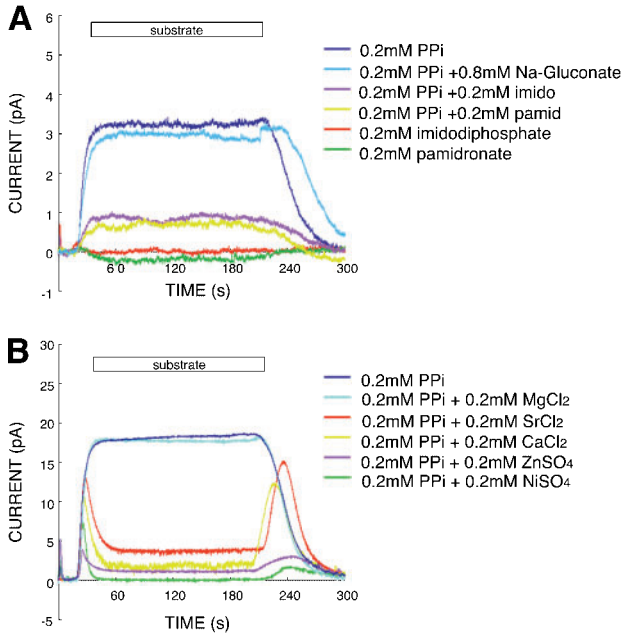


Fig. 4. **Effects of various agents on $H^+$-PPase activity.** (A) Inhibition of $PP_i$-dependent currents by non-hydrolysable $PP_i$ analogues (imido, imidodiphosphate; pamid, pamidronate). (B) Inhibition of $PP_i$-dependent currents by metal ions. $Sr^{2+}$, $Ca^{2+}$, $Zn^{2+}$ or $Ni^{2+}$ (0.2 mM) was added to the bathing solution containing 0.2 mM $PP_i$ and 1 mM $Mg^{2+}$.

firmed that the $PP_i$-induced current was caused by $H^+$-PPase.

$Ca^{2+}$ reversibly inhibits $H^+$-PPase through the formation of a Ca-PPi complex that competes with the substrate (Mg-$PP_i$) or with the interaction of free $Ca^{2+}$ and the enzyme (*9*). $Sr^{2+}$, $Zn^{2+}$ and $Ni^{2+}$ inhibited the $H^+$ pump activity of $H^+$-PPase even in the presence of 1 mM $Mg^{2+}$ as well as $Ca^{2+}$ (Fig. 4B). Further addition of $Mg^{2+}$ (final concentration, 1.2 mM) did not affect the current, indicating that the inhibition was not due to a concentration-dependent effect of metal ions. In the case of the addition of $Ca^{2+}$ and $Sr^{2+}$, exchange of the buffer transiently caused a peak current. The formation of the peak current is due to dilution of the inhibitory metal ion at the front of the medium flow in the tube connected to the patch-clamp apparatus.

*Dependence of the Current on the $PP_i$ Concentration*—Patch-clamp analysis allowed us to determine the $H^+$-

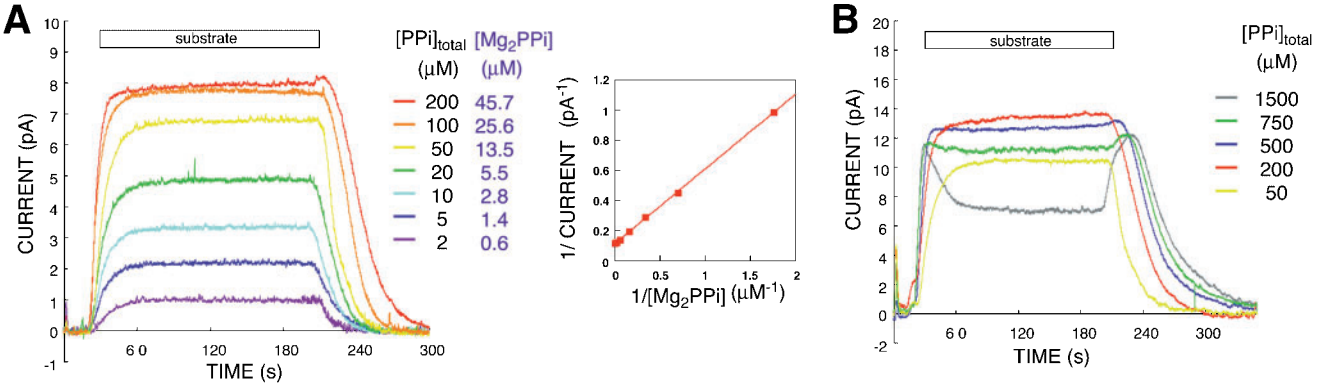


Fig. 5. **$PP_i$-dependent currents at various $Mg_2PP_i$ concentrations.** (A) The $H^+$ current was monitored using a single vacuole with the indicated concentrations of $PP_i$ (< 200 μM). (Right panel) Double reciprocal plots of steady-state currents versus $Mg_2PP_i$ concentration ($K_m$, 4.6 μM). The $Mg_2PP_i$ complex concentration ([$Mg_2PP_i$]) was calculated from the total concentrations of ([$PP_i$]$_{total}$), 1 mM $Mg^{2+}$ and 100 mM $K^+$ at pH7.5 (*26*). (B) Effect of the concentration (>500 μM) of $PP_i$.

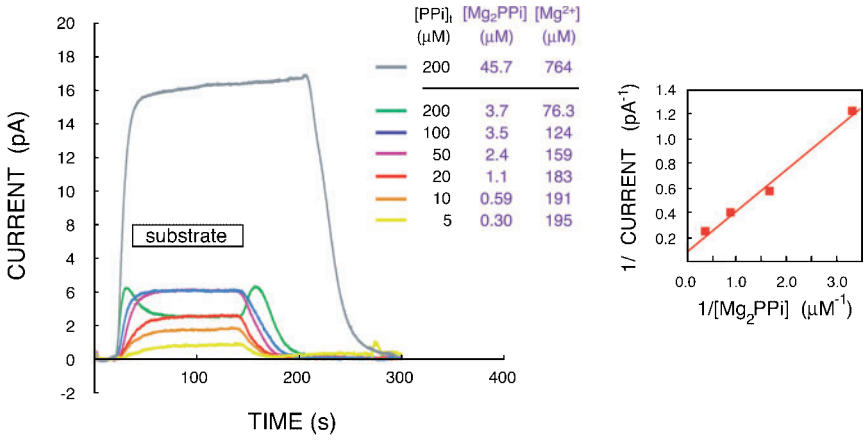


Fig. 6. **Current induced by $PP_i$ under low $Mg^{2+}$ conditions.** Whole-vacuole analysis was performed under the standard conditions (top line; 1 mM $MgCl_2$) or low $Mg^{2+}$ conditions (other lines, 0.2 mM $MgCl_2$). The current was recorded with various concentrations of PPi ($[PP_i]_{total}$). The apparent $K_m$ (4.4 μM) for $Mg_2PP_i$ was calculated from the double-reciprocal plot (right panel).

PPase activity in the same vacuole with various substrate concentrations (Fig. 5). The steady-state current increased in a concentration-dependent manner at low PPi concentrations and reached a maximum at 0.1 mM $PP_i$. An actual substrate for $H^+$-PPase is the $Mg_2PP_i$ complex (*26*). A double-reciprocal plot of current versus concentration of $Mg_2PP_i$ was linear (Fig. 5A, right panel). This relationship indicated that the $H^+$-PPase reaction follows Michaelis-Menten kinetics. The relationship between the concentration of $Mg_2PP_i$ ($[Mg_2PP_i]$) and the current ($I$) can be expressed as:

$$I = I_{max} [Mg_2PP_i] / (K_m + [Mg_2PP_i])$$

The $K_m$ value was determined in five separate experiments (4.6 ± 0.3 μM) (mean ± SD).

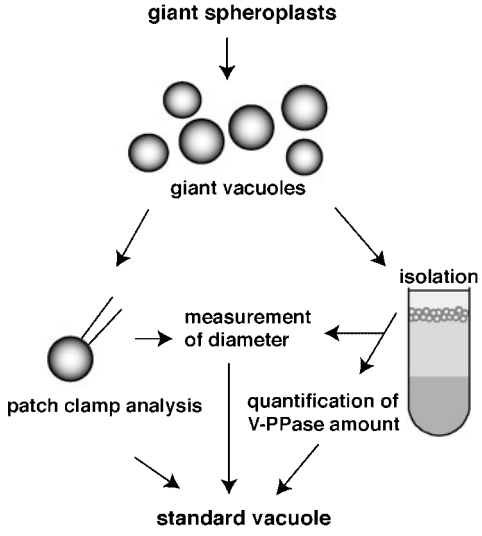


Fig. 7. **Determine the $H^+$-PPase amount in giant vacuoles.** Giant yeast vacuoles prepared from giant spheroplasts were used for patch-clamp analysis of $H^+$-PPase and immunochemical determination of the $H^+$-PPase amount. The diameters of the vacuoles were also determined before both experiments. The mean diameter of vacuoles used for patch-clamp analysis was 16.8 μm. Thus, a vacuole of this size was used as a model vacuole for calculation of the $H^+$-PPase amount in a single vacuole ($4.2 \times 10^6$ molecules per vacuole, see Table 1).

High concentrations of $PP_i$ reduced the $H^+$ transport current as shown with 1.5 mM $PP_i$ (Fig. 5B). This may be due to the imbalance between $PP_i$ and $Mg^{2+}$ for $Mg_2PP_i$ formation, and the decrease in the free concentration of $Mg^{2+}$, which is necessary for the formation of Mg-$PP_i$ complexes. Free $Mg^{2+}$ is essential for activation and stabilization of the enzyme (*9*, *17*). The $H^+$ current increased immediately after the supply of substrate and then dropped to a steady-state level. The formation of a peak current with 1.5 mM $PP_i$, immediately after substrate supply, is due to the dilution of $PP_i$ at the front of the medium flow in the tube. This shoulder was also observed after the substrate had been washed out (Fig. 5B).

Then we determined the $H^+$ current of $H^+$-PPase with a low concentration of $Mg^{2+}$ in the bathing buffer. Figure 6 shows the critical effect of a deficiency of $Mg^{2+}$ on the $H^+$ current. Under the conditions used ($PP_i$, 0.2 mM; $MgCl_2$, 0.2 mM), the current was 15% of the maximum current ($PP_i$, 0.2 mM, $MgCl_2$, 1 mM). The $K_m$ value for $Mg_2PP_i$ was calculated to be 4.4 μM under the conditions used ($MgCl_2$, 0.2 mM; $PP_i$, 5 to 50 μM). The value is the same as that (4.6 μM) in the presence of 1 mM $MgCl_2$ (Fig. 5A). The $H^+$ current was decreased with 0.1 and 0.2 mM $PP_i$ (Fig. 6). This may be due to the decrease in the concentration of free $Mg^{2+}$.

Table 1. **$H^+$ transport rate of $H^+$-PPase determined by the patch-clamp technique.**

| Parameter | Value | SE (*n*) |
|---|---|---|
| $PP_i$-induced current (fA/μm²)[a] | 10.5 | 1.06 (13) |
| Vacuole diameter (μm) | 16.8 | 0.50 (50) |
| Amount of $H^+$-PPase (pg/vacuole)[b] | 0.56 | 0.083 (3) |
| Surface area of model vacuole (μm²)[c] | 885 | |
| $PP_i$-induced current of model vacuole (pA)[c] | 9.3 | |
| $H^+$-PPase number (per vacuole)[c] | $4.2 \times 10^6$ | |
| Current per enzyme (pA) | $2.2 \times 10^{-6}$ | |
| Turnover number (per s) | 14 | |

[a]Steady state currents induced by $PP_i$ (0.2 mM) were recorded in the whole-vacuole mode. The current was normalized as to the surface area of an individual vacuole calculated from the diameter. [b]Giant vacuoles were isolated from protoplasts for quantification of $H^+$-PPase. The amount of $H^+$-PPase in the giant vacuole fraction was measured by immunoblotting. The specific content of $H^+$-PPase per vacuole was calculated from the amount of enzyme and the number of vacuoles in the fraction. [c]A vacuole with a diameter of 16.8 μm was treated as a model vacuole.

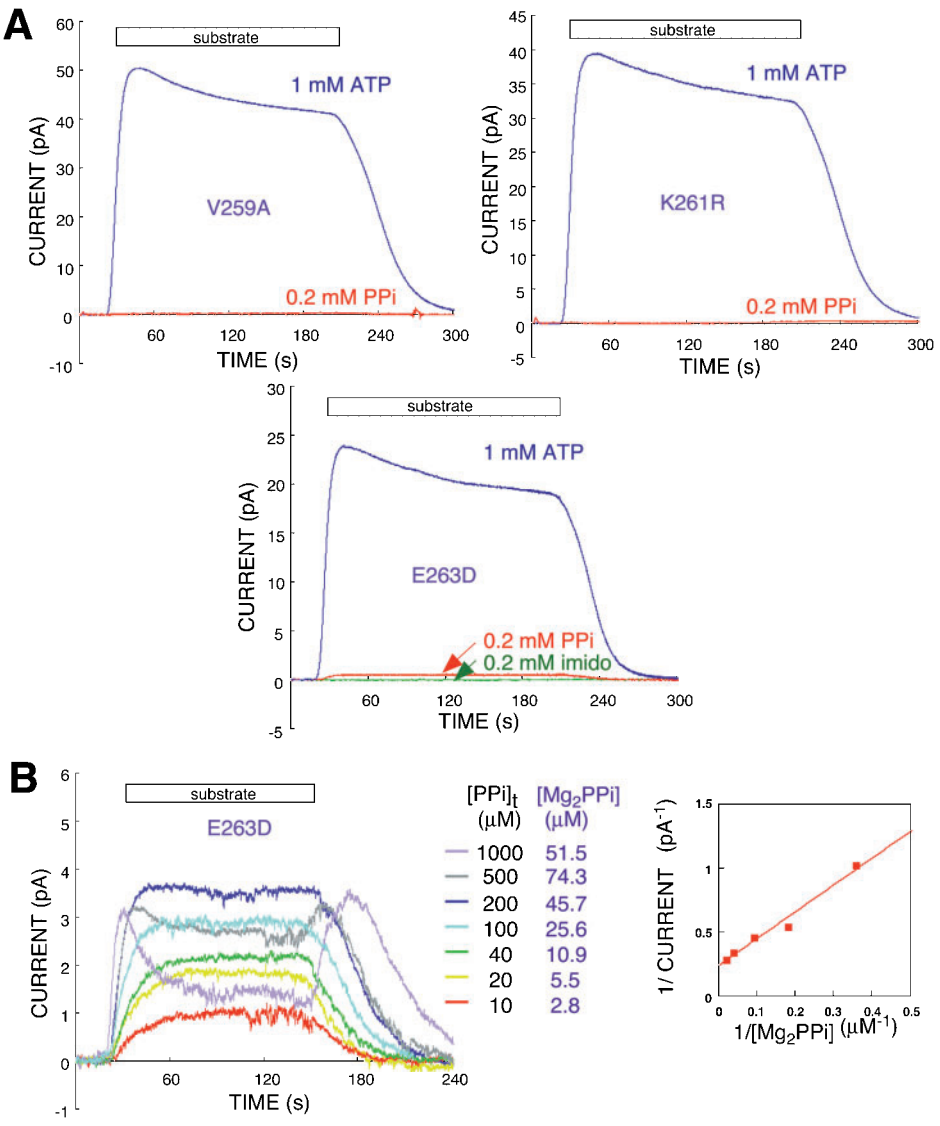


Fig. 8. **Proton pump activities of H⁺-PPase mutants.** (A) PPi-induced currents in vacuoles expressing H⁺-PPase mutants (V259A, K261R, and E263D). (B) Affinity of H⁺-PPase mutant E263D for $Mg_2PP_i$. Whole-vacuole currents were recorded at the indicated concentrations of $[PP_i]_{total}$. The apparent $K_m$ (10.6 μM) of E263D for $Mg_2PP_i$ was calculated from the double-reciprocal plot (right panel).

*Quantification of H⁺-PPase in Isolated Vacuoles*—It is difficult to determine the turnover number in patch-clamp experiments because the $PP_i$-induced current varies with the size of vacuole and the amount of H⁺-PPase. We therefore combined patch-clamp analysis with biochemical quantification of the enzyme, as shown in Fig. 7. The diameters of 50 giant vacuoles were measured. A mean diameter of 16.8 μm was used for a model vacuole. The amount of H⁺-PPase in giant vacuoles was determined using a specific antibody to H⁺-PPase and the purified enzyme. The mean H⁺-PPase amount for this model vacuole was 0.56 pg (Table 1). From these values and the molecular mass of the enzyme (80 kDa), the mean H⁺-PPase number in a model vacuole with a diameter of 16.8 μm was calculated to be $4.2 \times 10^6$ molecules.

*Determination of the Proton Pump Activities of Mutant Enzymes*—We also recorded the activities of three mutants of uncoupling-type H⁺-PPase, V259A (Val-259 exchanged with Ala), K261R, and E263D (Fig. 8A). The protein amounts of mutant H⁺-PPases accumulated in yeast vacuolar membrane were similar to the wild-type enzyme. These mutant enzymes hydrolyzed PPi (activity, 28–56% of wild type enzyme), but hardly exhibited the H⁺ pump activity (*17*). However, the E263D mutant, but not the V259A or K261R mutant, of H⁺-PPase generated $PP_i$-dependent currents of 1–3 pA (Fig. 8A). The current depended on the $PP_i$ concentration (Fig. 8B) and was not induced by imidodiphosphate, a PPi analogue (Fig. 8A). The apparent $K_m$ of the E263D mutant enzyme was 10.6 ± 1.6 μM (Fig. 8B). The affinity of the mutant enzyme was lower than the wild-type enzyme (4.6 μM). The results provide kinetic evidence that the Glu-263 of mung bean enzyme is involved in the binding of a substrate. It should be noted that kinetic parameters of the H⁺-PPase mutants could not be determined from the PPi hydrolysis activity in membranes prepared from yeast, since their activities were low and the background activity was relatively high.

## DISCUSSION

*Kinetic Parameters and Biochemical Properties Determined by Patch-Clamp Analysis of Heterologously Expressed H⁺-PPase*—This is the first examination of patch-clamp analysis of the ion pump expressed in heterologous species. We established the conditions, such as a promoter (GAP promoter), plasmid (pYN10), and yeast strain (BJ5458), for high efficient expression of H⁺-PPase in yeast. The method for preparation of giant yeast cells was that developed previously for patch clamp analysis of endogenous V-ATPase (*6*), except for the use of Aculeacin A as an inhibitor of the yeast cell wall synthesis instead of 2-deoxy glucose to prepare giant yeast cells, in which H⁺-PPase was highly accumulated. Under these conditions, we could obtain stable giant vacuoles and monitor the stable H⁺ currents of H⁺-PPase by whole vacuole patch-clamp configuration.

By patch-clamp recording, enzyme activity can be monitored for a long period. Furthermore, the assay medium can be kept at the initial conditions, since new reaction medium is constantly supplied to the bath. The $K_m$ value for $Mg_2PP_i$ was determined to be 4.6 μM (Fig. 5). This value is comparable to the $PP_i$-hydrolysis activity of H⁺-PPase in vacuolar membranes prepared from mung bean hypocotyls (4.9 μM) (*26*). The consistency of the $K_m$ values determined for $PP_i$ hydrolysis and H⁺ current means that PPi hydrolysis is tightly coupled to active transport of H⁺ through vacuolar membranes.

To determine the molecular activity of H⁺-PPase, we measured the diameter of giant vacuoles and the H⁺ current, and quantified the H⁺-PPase protein (Table 1). A vacuole with a mean diameter of 16.8 μm was used as a model vacuole, which is approximately 10-times larger than the vacuoles in normal yeast. The amount of H⁺-PPase protein in isolated giant vacuoles was determined immunochemically and the mean H⁺-PPase number in the model vacuole was calculated to be $4.2 \times 10^6$ molecules. The $PP_i$-induced current at 0.2 mM $PP_i$ was determined and normalized as to the surface area of each vacuole (Table 1). The obtained value (10.5 fA/μm²) is twice the reported value for vacuoles isolated from sugar beet taproot (5 fA/μm²) (*2*). A H⁺-PPase molecule is calculated to generate a current of $2.2 \times 10^{-6}$ pA. A current of 1 pA for H⁺ represents a turnover number of $6.24 \times 10^6$ ions/s. Thus, the H⁺ transport rate of H⁺-PPase per single molecule can be calculated to be 14 $s^{-1}$. Since H⁺-PPase exists as a homodimer (*9*, *18*, *27*), the molecular activity of the dimer is 28 $s^{-1}$. This value is comparable to the PPi-hydrolysis activity of the purified enzyme (33 $s^{-1}$) (*28*) and indicates a $H^+/PP_i$ stoichiometry of 1.

This is the first determination of the ion transport activity of a mutated ion pump by means of the patch-clamp technique. We chose three mutants of H⁺-PPase (V259A, K261R, and E263D), which hydrolyzed PPi but hardly transported H⁺ across the membrane. These residues are located in the main cytosolic loop (*17*). The H⁺ pump activities of these mutant enzymes could not be detected with a conventional method, however, the present technique enabled us to detect the H⁺ current of E263D and to determine its high $K_m$ value (Fig. 8). The E263A mutant exhibits neither $PP_i$-hydrolysis nor H⁺-transport activity, as reported previously (*17*). Thus the acidic residue at position 263 is essential for the PPi hydrolysis function, and exchange to an Asp residue markedly reduces the affinity for a substrate. On the other hand, no H⁺ current was detected for the V259A and K261R mutants with the present method with high resolution. The results suggest that these two residues are essential for energy transfer from $PP_i$ hydrolysis to H⁺ translocation across the membrane.

In conclusion, the most reliable kinetic properties of H⁺-PPase were obtained in the present study by patch-clamp analysis of the heterologously expressed enzyme. Furthermore, this is the first demonstration of transient peak activity under some conditions, such as the co-existence of metal ions (Fig. 4B), the presence of an excess amount of $PP_i$ (Fig. 5B), and a deficiency of $Mg^{2+}$ (Fig. 6).

*Advantages of the Present Method*—Conventionally, the proton pumping activities of $PP_i$-, ATP-, and other energy-driven proton pumps have been indirectly measured by the fluorescence quenching method, an outline of which follows. (i) The pumps transport H⁺ the membrane vesicles and generate a pH gradient. (ii) The ΔpH drives the movement of a basic, ΔpH-sensitive fluorescent dye, such as acridine orange, into the vesicles. (iii) The dye concentrated in small vesicles loses fluorescence through auto-quenching. The quantitative measurement of activity is difficult because of this complex reaction mechanism; that is, ΔpH reflects not only the pump activity but also the activity of ΔpH driven by secondary transporters and the size of the vesicles. Substrates, inhibitors (*e.g.* $Ni^{2+}$), and natural fluorescent pigments in the membrane often interfere with the fluorescent intensity of the dye. Inconsistent kinetic constant values between substrate hydrolysis and H⁺ pumping activities may be due to these measurement problems.

The present study directly demonstrated that H⁺-PPase acts as a stable proton pump with a turnover number of 14 $s^{-1}$ and a $K_m$ for $Mg_2PP_i$ of 4.6 μM. The enzyme translocates H⁺ at a constant rate, over more than 3 min, and the same rate can be monitored reproducibly with the same vacuole after intervals of several minutes. This method has many advantages. It can be used for the functional analysis of ion pumps and transporters exogenously expressed in yeast. The use of an efficient expression vector and yeast mutant strains without proteinases can increase the accumulation of exogenous proteins. It is easy to obtain mutants that lack specific transporters and ion channels in order to diminish background activity. Although normal yeast cells are small and bounded by a tough cell wall, isolated giant vacuoles can be penetrated by microelectrodes to monitor transporter-mediated currents. Heterologous expression of mRNA in immature eggs (oocytes) of *Xenopus laevis* provides a system for characterizing membrane proteins. It takes several days to express the target proteins in oocytes. The endogenous transporter activity detected varies with the batch and stage of oocyte development. Genetic manipulation of endogenous channels and transporters is also rather difficult.

Presently, it is hard to control the intracellular localization of membrane proteins, which are heterologously expressed in yeast cells. However, there is a possibility that all types of membrane proteins are localized in the vacuolar membrane under the artificial conditions of

overexpression. Some mutant strains of yeast, whose secretory pathways are confusing, can be used as host cells for the heterologous expression of membrane proteins. Mutants, such as *vma1* and *lcb1*, missort the endogenous plasma membrane $H^+$-ATPase (Pma1p) to the vacuolar membrane (*29*, *30*). Thus, our technique can be applied to any transporter localized to any membrane system in original host cells.

The present method will become an important tool for functional genomics, since the functions of many genes encoding membrane transport systems, identified in human (*31*) and *A. thaliana* (*32*), remain unknown. By expressing a protein in an appropriate yeast strain, activity can be monitored as a membrane current under various bathing medium conditions. The whole-giant-vacuole clamp technique may be one of the most reliable methods for identifing unknown ion transporters. Furthermore, this method may yield essential information on missense mutations of ion transporters that cause genetic diseases such as Hailey-Hailey (mutation in the endomembrane type $Ca^{2+}$-ATPase) (33) and Menkes disease ($Cu^{2+}$-ATPase) (*34*).

We wish thank Hisatoshi Mimura for providing the purified $H^+$-PPase. Y.N. received a research fellowship from the Japan Society for the Promotion of Science for Young Scientists. This work was supported by grants from the Japanese Ministry of Education, Science, Sports and Culture for Scientific Research on Priority Areas (Nos. 10219203 and 13142203) and COE Research (13CE2005).

## REFERENCES

1. Neher, E. and Sakmann, B. (1976) Single-channel currents recorded from membrane of denervated frog muscle fibres. *Nature* **260**, 799–802
2. Hedrich, R., Kurkdjian, A., Guern, J., and Flügge, U.I. (1989) Comparative studies on the electrical properties of the $H^+$ translocating ATPase and pyrophosphatase of the vacuolar-lysosomal compartment. *EMBO J.* **8**, 2835–2841
3. Neher, E. and Sakmann, B. (1992) The patch clamp technique. *Sci. Amer.* **266**, 44–51
4. Bertl, A., Anderson, J.A., Slayman, C.L., and Gaber, R.F. (1995) Use of *Saccharomyces cerevisiae* for patch-clamp analysis of heterologous membrane proteins: characterization of Kat1, an inward-rectifying $K^+$ channel from *Arabidopsis thaliana*, and comparison with endogenous yeast channels and carriers. *Proc. Natl. Acad. Sci. USA* **92**, 2701–2705
5. Kuroda, T., Okuda, N., Saitoh, N., Hiyama, T., Terasaki, Y., Anazawa, H., Hirata, A., Mogi, T., Kusaka, I., Tshuchiya, T., and Yabe, I. (1998) Patch clamp studies on ion pumps of the cytoplasmic membrane of *Escherichia coli*. Formation, preparation, and utilization of giant vacuole-like structures consisting of everted cytoplasmic membrane. *J. Biol. Chem.* **273**, 16897–904
6. Yabe, I., Horiuchi, K., Nakahara, K., Hiyama, T., Yamanaka, T., Wang, P.C., Toda, K., Hirata, A., Ohsumi, Y., Hirata, R., Anraku, Y., and Kusaka, I. (1999) Patch clamp studies on V-type ATPase of vacuolar membrane of haploid *Saccharomyces cerevisiae*: preparation and utilization of a giant cell containing a giant vacuole. *J. Biol. Chem.* **274**, 34903–34910
7. Baltscheffsky, M., Nadanaciva, S., and Schultz, A. (1998) A pyrophosphate synthase gene: molecular cloning and sequencing of the cDNA encoding the inorganic pyrophosphate synthase from *Rhodospirillum rubrum*. *Biochim. Biophys. Acta* **1364**, 301–306
8. Scott, D.A., de Souza, W., Benchimol, M., Zhong, L., Lu, G.G., Moreno, S.N.J., and Docampo, R. (1998) Presence of a plant-like proton-pumping pyrophosphatase in acidocalcisomes of *Trypanosoma cruzi*. *J. Biol. Chem.* **273**, 22151–22158
9. Maeshima, M. (2000) Vacuolar $H^+$-pyrophosphatase. *Biochim. Biophys. Acta* **1465**, 37–51
10. Drozdowicz, Y.M. and Rea, P.A. (2001) Vacuolar $H^+$ pyrophosphatases: from the evolutionary backwaters into the mainstream. *Trends Plant Sci.* **6**, 206–211
11. Ruiz, F.A., Marchesini, N., Seufferheld, M., Govindjee, and Docampo, R. (2001) The polyphosphate bodies of *Chlamydomonas reinhardtii* posses a proton-pumping pyrophosphatase and are similar to acidocalcisomes. *J. Biol. Chem.* **276**, 46196–46203
12. Mitsuda, N., Enami, K., Nakata, M., Takeyasu, K., and Sato, M.H. (2001) Novel type *Arabidopsis thaliana* $H^+$-PPase is localized to the Golgi apparatus. *FEBS Lett.* **488**, 29–33
13. Belogurov, G.A., Turkina, M.V., Penttinen, A., Huopalahti, S., Baykov, A.A., and Lahti, R. (2002) $H^+$-pyrophosphatase of *Rhodospirillum rubrum*. High yield expression in *Escherichia coli* and indentification of the Cys residues responsible for inactivation by mersalyl. *J. Biol. Chem.* **277**, 22209–22214
14. Saliba, K.J., Allen, R.J.W., Zissis, S., Bray, P.G., Ward, S.A., and Kirk, K. (2003) Acidification of the malarian parasite's digestive vacuole by a $H^+$-ATPase and a $H^+$-pyrophosphatase. *J. Biol. Chem.* **278**, 5605–5612
15. Davies, J.M., Poole, R.J., and Sanders, D. (1993) The computed free energy change of hydrolysis of inorganic pyrophosphate and ATP: apparent significance for inorganic-pyrophosphate-driven reactions of intermediary metabolism. *Biochim. Biophys. Acta* **1141**, 29–36
16. Maeshima, M. (2001) Tonoplast transporters: organization and function. *Annu. Rev. Plant Physiol. Plant Mol. Biol.* **52**, 469–497
17. Nakanishi, Y., Saijo, T., Wada, Y., and Maeshima, M. (2001) Mutagenic analysis of functional residues in putative substrate-binding site and acidic domains of vacuolar $H^+$-pyrophosphatase. *J. Biol. Chem.* **276**, 7654–7660
18. Tanaka, K., Nakafuku, M., Tamanoi, F., Kaziro, Y., Matsumoto, K., and Toh-e, A. (1990) IRA2, a second gene of *Saccharomyces cerevisiae* that encodes a protein with a domain homologous to mammalian ras GTPase-activating protein. *Mol. Cell. Biol.* **10**, 4303–4313
19. Nakanishi, Y. and Maeshima, M. (1998) Molecular cloning of vacuolar $H^+$-pyrophosphatase and its developmental expression in growing hypocotyl of mung bean. *Plant Physiol.* **116**, 589–597
20. Gietz, R.D., Schiestl, R.H., Willems, A.R., and Woods, R.A. (1995) Studies on the transformation of intact yeast cells by the LiAc/ss-DNA/PEG procedure. *Yeast* **11**, 355–360
21. Osumi, M. (1998) The ultrastructure of yeast: cell wall structure and formation. *Micron* **29**, 207–233
22. Ohsumi, Y. and Anraku, Y. (1981) Active transport of basic amino acids driven by a proton motive force in vacuolar membrane vesicles of *Saccharomyces cerevisiae*. *J. Biol. Chem.* **256**, 2079–2082
23. Maeshima, M. and Yoshida, S. (1989) Purification and properties of vacuolar membrane proton-translocating inorganic pyrophosphatase from mung bean. *J. Biol. Chem.* **264**, 20068–20073
24. Faulkner, J.D.B., Anson, J.G., Tuite, M.F., and Minton, N.P. (1994) High-level expression of the phenylalanine ammonia lyase-encoding gene from *Rhodosporidium toruloides* in *Saccharomyces cerevisiae* and *Escherichia coli* using a bifunctional expression system. *Gene* **142**, 13–20
25. Zhen, R.G., Baykov, A.A., Bakuleva, N.P., and Rea, P.A. (1994) Aminomethylenediphosphonate: a potent type-specific inhibitor of both plant and phototrophic bacterial $H^+$-pyrophosphatases. *Plant Physiol.* **104**, 153–159
26. Baykov, A.A., Bakuleva, N.P., and Rea, P.A. (1993) Steady-state kinetics of substrate hydrolysis by vacuolar $H^+$-pyrophosphatase: a simple three-state. *Eur. J. Biochem.* **217**, 755–762

27. Sato, M.H., Maeshima, M., Ohsumi, Y., and Yoshida, M. (1991) Dimeric structure of $H^+$-translocating pyrophosphatase from pumpkin vacuolar membranes. *FEBS Lett.* **290**, 177–180
28. Ueoka-Nakanishi, H. and Maeshima, M. (2001) Quantification of $Ca^{2+}/H^+$ antiporter VCAX1p in vacuolar membranes and its absence in roots of mung bean. *Plant Cell Physiol.* **41**, 1067–1071
29. Hirata, R. and Takatsuki, A. (2001) Role of organelle acidification in intracellular protein transport. *RIKEN Rev.* **41**, 90–91
30. Bagnat, M., Chang, A., and Simons, K. (2001) Plasma membrane proton ATPase Pma1p requires raft association for surface delivery in yeast. *Mol. Biol. Cell.* **12**, 4129–4138
31. International Human Genome Sequencing Consortium (2001) Initial sequencing and analysis of the human genome. *Nature* **409**, 860–921
32. The Arabidopsis Genome Initiative (2000) Analysis of the genome sequence of the flowering plant Arabidopsis thaliana. *Nature* **408**, 796–815
33. Hu, Z., Bonifas, J.M., Beech, J., Bench, G., Shigihara, T., Ogawa, H., Ikeda, S., Mauro, T., and Epstein, E.H. Jr. (2000) Mutations in ATP2C1, encoding a calcium pump, cause Hailey-Hailey disease. *Nature Genet.* **24**, 61–65
34. Harris, E.D., Reddy, M.C., Qian, Y., Tiffany-Castiglioni, E., Majumdar, S., and Nelson, J. (1999) Multiple forms of the Menkes Cu-ATPase. *Adv. Exp. Med. Biol.* **448**, 39–51